Quantum images and critical fluctuations in the optical parametric oscillator below threshold

A. Gatti and L. Lugiato
Dipartimento di Fisica dell'Università, Via Celoria 16 20133, Milano Italy
(Received 18 January 1995)

In the first part of the paper we define the spatial spectrum of squeezing following an operational procedure, and we show in general how the spatial structure of squeezed states can be described in terms of correlation functions of quadrature components of the electric field. In the second part we formulate an appropriate quantum model for a degenerate optical parametric oscillator (OPO) with plane mirrors, and we analyze it extensively below the threshold for signal generation The correlation length diverges when the OPO approaches threshold; this picture provides an ideal completion of the analogy with critical phenomena in second-order phase transition at equilibrium. The spatial configuration of the correlation function exhibits the phenomenon of "quantum image:" the signal field, which is purely generated by quantum noise, shows an ordered spatial structure which is observable via the spatial correlation function.

PACS number(s): 42.50.Dv, 42.65.−k

I. INTRODUCTION

In the last few years our group activated a research line which aims at unifying the two fields of transverse nonlinear optics and of squeezing. The first discipline studies the phenomena of pattern formation and transformation, which arise in the structure of the electromagnetic field in the planes orthogonal to the direction of propagation [1–4]. The second studies the nonclassical states of the radiation field and the procedure to obtain quantum noise reduction and application thereof [5–7]. With respect to theory, the two fields exhibit traditionally a complementary situation: in transverse nonlinear optics models are two or three dimensional in space, but only semiclassical, whereas in the domain of squeezing, with few pioneering exceptions [8–12], theoretical treatments are fully quantum but at most one dimensional in space because of the plane wave approximation, which ensures that the electric field is uniform in the transverse plane. In the last two years we started analyzing theories which are at the same time quantum mechanical and multidimensional in space; this approach activated, on the one hand, the analysis of quantum effects in nonlinear optical patterns [13–15] and, on the other, the study of the spatial structure of squeezed states [16].

This paper starts from the analysis reported in [16] where, in particular, we showed that the description of the spatial structure of squeezed states requires consideration of a local oscillator field (LOF) with an arbitrary spatial configuration in the transverse plane. This situation, however, cannot be easily realized in a laboratory. We show in this paper that the spectrum of squeezing, defined in [16] for a LOF of arbitrary shape, can be unequivocally expressed in terms of the space-time correlation function of the electric field. This implies that by measuring the spatial correlation function [e.g., by a pair of pointlike detectors with variable position or using a charge-coupled device (CCD) camera] with a fixed LOF, available in the laboratory, it is possible to obtain the level of squeezing which would be measured in any experiment which utilizes a LOF with the same spatial phase distribution (modulo π) of the actually used LOF, but with an arbitrary spatial intensity distribution. This implies, expecially, that by using a single LOF, and measuring the spatial correlation function of the electric field as described below, it is possible to obtain the whole spectrum of squeezing without need of changing the spatial configuration of the LOF itself.

This analysis allows us also to establish formally the relation between our approach and that of Kolobov and Soklov. As a matter of fact, Kolobov and Sokolov [10] started their analysis just from consideration of the space-time correlation function, and defined the spectrum of squeezing as the space-time Fourier transform of the correlation function. In our theory, instead, we pursue an operational approach and start from the very definition of the spectrum of squeezing, which arises from a balanced homodyne detection procedure. We briefly discuss also the case of the spectrum of the intensity fluctuations.

While the first part of the paper is general, in the second part we perform an analytical calculation of the space-time correlation function (as well as of its Fourier transform in space and time) in the case of the degenerate optical parametric oscillator (OPO) below threshold, in a plane mirror configuration. In this way, we can describe the critical behavior of the quantum fluctuations, and the divergence of the correlation length, when the OPO threshold is approached. These kinds of phenomena are analyzed here in the case of a quantum system far from thermal equilibrium and, especially, in the case of an optical system. In addition, these results provide an essential completion of the classic analogy between lasers (as well as other nonlinear optical systems such as, e.g., OPO's) and second-order phase transitions in equilibrium systems [17–19].

Another relevant aspect of this paper is related to the

analysis of Ref. [23], which shows that, for negative values of the detuning parameter, the signal field of the OPO above threshold is generated in the form of a stripe pattern instead of a uniform distribution. We show here that, for the same values of the detuning parameter but with the OPO *below* threshold, the spatial correlation function of the electric field exhibits the same spatial modulation which characterizes the intensity distribution when the OPO is above threshold. Below threshold, however, the intensity and phase configuration are perfectly uniform on average. Therefore, we have a "quantum image" [15], because the spatial structure does not appear in the intensity configuration, but in the spatial correlation function of the quantum fluctuations. In this way, we follow the same nomenclature and the same "spirit" as Knight and collaborators [24], who develop the idea of encoding information in the spatial correlation function of the electric field, rather than in the intensity distribution.

We mention that, under appropriate conditions, the "quantum image" phenomenon can appear also above threshold; this result, together with the general definition of quantum image, is discussed in [15].

In Sec. II we define the spectrum of squeezing obtained using a LOF of arbitrary spatial configuration; in Sec. III we express this spectrum in terms of an appropriate spatial correlation function. Attention is paid also to the finite size of the detectors used to measure the correlation function. Section IV discusses, instead, the spectrum of the intensity fluctuations in the case that the mean value of the field is much larger than its fluctuations. In Sec. V we introduce the quantum model for the OPO, and in Sec. VI we summarize the pattern formation phenomena which emerge from the semiclassical approximation of this model. The angular dependence of the level of squeezing is discussed in general in Sec. VII. Starting from Sec. VIII, we focus on the OPO below threshold. The correlation function is discussed in the temporal domain in Sec. IX and in the spatial domain in Sec. X; in particular, we emphasize the critical behavior of the quantum fluctuations observed approaching the OPO threshold, and the concept of quantum image. The final section summarizes the results of the paper.

II. BALANCED HOMODYNE DETECTION AND SPATIAL STRUCTURE OF SQUEEZED STATES

Let us consider the well known balanced homodyne detection scheme for squeezed states [5] (Fig. 1). The beam splitter combines the quantum field $A_{out}(\mathbf{x},t)$ and the local oscillator field (LOF) which lies in a classical, stationary, coherent state $\alpha_L(\mathbf{x})$ of intensity much larger than that of A_{out}; here $\mathbf{x}=(x,y)$ denotes the position vector in the plane orthogonal to the direction of propagation of the field, and A_{out} is a free field envelope operator which obeys the commutation rule

$$\left[A_{out}(\mathbf{x},t),A^{\dagger}_{out}(\mathbf{x}',t')\right]=\delta(\mathbf{x}-\mathbf{x}')\delta(t-t')\;; \qquad (1)$$

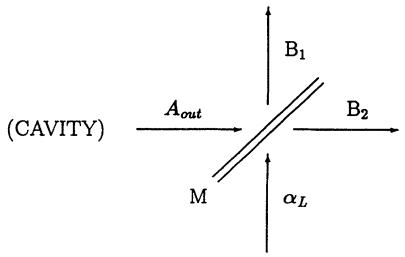

FIG. 1. Balanced homodyne detection scheme. The mirror M has transmission and reflection coefficients $t=r=1/\sqrt{2}$.

$|\alpha_L|^2$ is expressed in $\mathrm{cm}^{-2}\ \mathrm{s}^{-1}$.

Assuming that the transmission and the reflection coefficients of the mirror M in Fig. 1 are given by $t=r=1/\sqrt{2}$, the fields B_1 and B_2 beyond the mirror are given by

$$B_1(\mathbf{x},t)=\frac{1}{\sqrt{2}}\left[A_{out}(\mathbf{x},t)+\alpha_L(\mathbf{x})\right] \qquad (2)$$

and

$$B_2(\mathbf{x},t)=\frac{1}{\sqrt{2}}\left[A_{out}(\mathbf{x},t)-\alpha_L(\mathbf{x})\right]\;. \qquad (3)$$

In balanced homodyne detection one measures the difference between the total powers of the two beams B_1 and B_2, which is given by

$$\int d^2\mathbf{x}\,\left[B_1^{\dagger}(\mathbf{x},t)B_1(\mathbf{x},t)-B_2^{\dagger}(\mathbf{x},t)B_2(\mathbf{x},t)\right] = N^{\frac{1}{2}}E_H^{out}(t)\;, \qquad (4)$$

where

$$E_H^{out}(t)=\frac{1}{N^{\frac{1}{2}}}\int d^2\mathbf{x}\left[\alpha_L(\mathbf{x})A^{\dagger}_{out}(\mathbf{x},t)+\alpha_L^{*}(\mathbf{x})A_{out}(\mathbf{x},t)\right]\;, \qquad (5)$$

$$N=\int d^2\mathbf{x}\;|\alpha_L(\mathbf{x})|^2\;. \qquad (6)$$

Thus the homodyne detection performs the projection of the field A_{out} onto the local oscillator field α_L. As shown in the Appendix, this fact can be utilized also to obtain the coefficients of the expansion of the mean value of A_{out} over an arbitrary set of orthonormal modes.

Here, however, we are interested in the quantum fluctuations around a stationary mean value. They are described by the spectrum

$$V(\omega)=\int_{-\infty}^{+\infty}dt\,e^{-i\omega t}\langle\delta E_H^{out}(t)\,\delta E_H^{out}(0)\rangle\;, \qquad (7)$$

where

$$\delta E_H^{out}(t)=E_H^{out}(t)-\langle E_H^{out}\rangle\;. \qquad (8)$$

By using Eqs. (5), (6), and (1), one obtains easily that

$$V(\omega) = 1 + S(\omega) , \tag{9}$$

with

$$S(\omega) = \int_{-\infty}^{+\infty} dt\, e^{-i\omega t} \langle : \delta E_H^{out}(t)\, \delta E_H^{out}(0) : \rangle , \tag{10}$$

where :: indicates normal and time ordering. The first term in the right hand side of Eq. (9) represents the shot noise level, which is normalized to 1. In the following we will call $S(\omega)$ the spectrum of squeezing. One has that $S(\omega) \geq -1$, and $S(\omega) = -1$ means that at frequency ω there is complete suppression of quantum noise in the observable E_H^{out}.

We are interested in the case that the field A_{out} is emitted by a nonlinear cavity with a single input-output mirror with reflection coefficient $r_c \approx 1$ and transmission coefficient $t_c = (1-r_c^2)^{\frac{1}{2}}$. In terms of the intracavity field $A(\mathbf{x}, t)$, the outgoing field $A_{out}(\mathbf{x}, t)$ is given by

$$A_{out}(\mathbf{x}, t) = \sqrt{2\gamma} A(\mathbf{x}, t) - A_{in}(\mathbf{x}, t) , \tag{11}$$

where $\gamma = ct_c^2/2\mathcal{L}$ is the cavity damping rate of the field, with $\mathcal{L}$ being the cavity round trip length, and A_{in} is the field incident onto the cavity, which is assumed to be in a coherent state (possibly in the vacuum state). The fields A_{out}, A, and A_{in} have the same carrier frequency. In writing Eq. (11) we have assumed that the homodyne detection takes place near the cavity, so that it is not necessary to take into account the evolution of the field from the cavity coupling mirror to the beam splitter M. Accordingly A in Eq. (11) denotes the intracavity field near the input-output port.

Next we insert Eq. (11) into Eq. (10); by taking into account that the input field A_{in} is in a coherent state and that the product in (10) is normally and time ordered, we have that A_{in} does not contribute to the expression (10) and

$$S(\omega) = 2\gamma \int_{-\infty}^{+\infty} dt\, e^{-i\omega t} \langle : \delta E_H(t)\, \delta E_H(0) : \rangle , \tag{12}$$

where

$$E_H(t) = A_H^\dagger(t) + A_H(t) , \tag{13a}$$

$$A_H(t) = \frac{1}{N^{\frac{1}{2}}} \int d^2\mathbf{x}\, \alpha_L^*(\mathbf{x}) A(\mathbf{x}, t) . \tag{13b}$$

Note that the operators A_H and $A_H^\dagger$ obey the harmonic oscillator commutation relation $[A_H(t), A_H^\dagger(t)] = 1$.

Since the homodyne detection provides only the projection of the quantum field onto the LOF $\alpha_L(\mathbf{x})$, in order to analyze the spatial structure of a squeezed state one must use local oscillator fields of different spatial configuration. Precisely, let us consider a complete orthonormal basis of functions $f_l(\mathbf{x})$, where l indicates an appropriate set of indices:

$$\int d^2\mathbf{x}\, f_l^*(\mathbf{x}) f_{l'}(\mathbf{x}) = \delta_{l,l'} . \tag{14}$$

Let us consider a LOF of the form

$$\alpha_L(\mathbf{x}) \propto f_l(\mathbf{x}) e^{i\theta} , \tag{15}$$

where θ is an arbitrary phase, and let us indicate by $S_l(\omega, \theta)$ the spectrum obtained with this choice; we call the set of functions $S_l(\omega, \theta)$ obtained by varying l the *spatial spectrum of squeezing*. Thus the spatial structure of a squeezed state is described by the infinite set of functions $S_l(\omega, \theta)$ and its observation requires using a LOF of variable spatial configuration.

In the case of a generic LOF, one can expand the quantum field $A(\mathbf{x}, t)$ on the basis f_l:

$$A(\mathbf{x}, t) = \sum_l f_l(\mathbf{x}) a_l(t) , \tag{16}$$

where, because of the commutation rule $[A(\mathbf{x}, t), A^\dagger(\mathbf{x}', t)] = \delta(\mathbf{x} - \mathbf{x}')$, one has

$$\left[a_l(t), a_{l'}^\dagger(t)\right] = \delta_{l.l'} . \tag{17}$$

By inserting Eq. (16) into Eqs. (13a) and (12), one obtains

$$S(\omega) = \sum_{l,l'} \rho_l \rho_{l'}\, S_{l,l'}(\omega) , \tag{18}$$

where we have set

$$\frac{1}{N^{\frac{1}{2}}} \int d^2\mathbf{x}\, \alpha_L^*(\mathbf{x}) f_l(\mathbf{x}) = \rho_l e^{-i\phi_l} \tag{19}$$

and

$$S_{l,l'}(\omega) = 2\gamma \int_{-\infty}^{+\infty} dt\, e^{-i\omega t} \langle : \delta A_l(t)\, \delta A_{l'}(0) : \rangle , \tag{20}$$

$$A_l = a_l^\dagger e^{i\phi_l} + a_l e^{-i\phi_l} . \tag{21}$$

In specific cases, as in the example of the OPO below threshold analyzed in the remainder of this paper, the operators a_l with different l are uncorrelated, and one obtains

$$S_{l,l'}(\omega) = S_l(\omega, \phi_l)\, \delta_{l,l'} \tag{22}$$

where $S_l(\omega, \phi_l)$ is just the spatial spectrum of squeezing defined above. Hence in this case one has the formula

$$S(\omega) = \sum_l \rho_l^2 S_l(\omega, \phi_l) , \tag{23}$$

which expresses the spectrum of squeezing for a generic LOF in terms of the spatial spectrum of squeezing. Note that $\sum_l \rho_l^2 = 1$.

We conclude this section with a remark concerning the observable E_H given by Eq. (13a). Let us express α_L in the form

$$\alpha_L(\mathbf{x}) = \rho_L(\mathbf{x}) e^{i\phi_L(\mathbf{x})},$$
$$\phi_L(\mathbf{x}) = \arg\left[\alpha_L(\mathbf{x})\right] \pmod{\pi} , \tag{24}$$

where the arbitrariness given by the specification (mod π) is included to allow, whenever possible, that the function $\rho_L(\mathbf{x})$ is continuous with its derivatives over the trans-

verse plane; hence $\rho_L(\mathbf{x})$ is real but not necessarily positive. With the position (24), the expression for E_H can be written as

$$E_H(\mathbf{x},t) = \frac{1}{N}\int d^2\mathbf{x}\,\rho_L(\mathbf{x})\mathcal{E}_H(\mathbf{x},t)\ , \tag{25}$$

$$\mathcal{E}_H(\mathbf{x},t) = A^\dagger(\mathbf{x},t)e^{i\phi_L(\mathbf{x})} + A(\mathbf{x},t)e^{-i\phi_L(\mathbf{x})}\ . \tag{26}$$

From this expression one sees explicitly that the homodyne detection picks up a quadrature component of the field; in general, however, the phase ϕ_L of the quadrature component is not constant over the transverse plane.

III. CONNECTION WITH THE SPATIAL CORRELATION FUNCTION

The main message of Ref. [16], and of the more detailed description given in the previous section, is that in order to explore the spatial structure of a squeezed state one must use a LOF with variable spatial configuration. In this section we illustrate an alternative method to measure the spectrum of squeezing $S(\omega)$ based on the spatial correlation function of the homodyne field. We will show that, using this method, one can obtain the spatial spectrum of squeezing $S_l(\omega,\theta)$ using only one LOF.

By inserting Eq. (25) into Eq. (12), one can express $S(\omega)$ at once in the form

$$S(\omega) = \frac{1}{N}\int_{-\infty}^{\infty} dt\,e^{-i\omega t}\int d^2\mathbf{x} \times \int d^2\mathbf{x}'\,\rho_L(\mathbf{x})\rho_L(\mathbf{x}')\,\Gamma(\mathbf{x},t;\mathbf{x}',0)\ , \tag{27}$$

where we have introduced the normally ordered spatiotemporal correlation function of the homodyne field, defined as

$$\Gamma(\mathbf{x},t;\mathbf{x}',0) = 2\gamma\langle{:}\,\delta\mathcal{E}_H(\mathbf{x},t)\,\delta\mathcal{E}_H(\mathbf{x}',0)\,{:}\rangle\ , \tag{28}$$

where $\mathcal{E}_H$ is defined by Eq. (26).

We note that the quantity

$$\Gamma_{\rho_L}(\mathbf{x},t;\mathbf{x}',0) = \rho_L(\mathbf{x})\rho_L(\mathbf{x}')\Gamma(\mathbf{x},t;\mathbf{x}',0) \tag{29}$$

is just the quantity obtained in a measurement of the space-time correlation function of the observable

$$B_1^\dagger(\mathbf{x},t)B_1(\mathbf{x},t) - B_2^\dagger(\mathbf{x},t)B_2(\mathbf{x},t)\ , \tag{30}$$

where B_1 and B_2 are the fields emerging from the homodyne detection [see Fig. 1 and Eqs. (2) and (3)].

Imagine, now, that we would like to measure, in our laboratory, the spectrum of squeezing $S_{\beta_L}(\omega)$ with the LOF β_L, but that only the LOF α_L is available. Provided that the two LOF's have the same phase distribution (mod π), i.e.,

$$\beta_L(\mathbf{x}) = \sigma_L(\mathbf{x})e^{i\phi_L(\mathbf{x})},\quad \alpha_L(\mathbf{x}) = \rho_L(\mathbf{x})e^{i\phi_L(\mathbf{x})}\ , \tag{31}$$

where σ_L and ρ_L are real, we can proceed as follows. We have

$$S_{\beta_L}(\omega) = \int_{-\infty}^{\infty} dt\,e^{-i\omega t}\int d^2\mathbf{x}\int d^2\mathbf{x}'\,\frac{\sigma_L(\mathbf{x})\sigma_L(\mathbf{x}')}{N} \times \Gamma(\mathbf{x},t;\mathbf{x}',0)\ . \tag{32}$$

The quantity $\Gamma(\mathbf{x},t;\mathbf{x}',0)$ can be obtained from measurements which utilize the available local oscillator α_L, by using Eq. (29) and the known configuration $\rho_L(\mathbf{x})$. Finally the spectrum $S_{\beta_L}(\omega)$ can be obtained numerically from Eq. (32) and from the known configuration $\sigma_L(\mathbf{x})$. This shows that, using a single LOF, it is possible to obtain the spectrum of squeezing corresponding to an arbitrary LOF with the same spatial phase distribution (modulo π).

Let us now turn our attention to the spatial spectrum $S_l(\omega,\theta)$. In order to obtain it, one should in principle measure all the squeezing spectra with the local oscillator field given by Eq. (15) for all possible choices of l. Assume that the only available LOF corresponds to one of these modes (for example, to the TEM_{00} mode of a complete set of Gauss-Laguerre modes), say

$$\alpha_L(\mathbf{x}) = C\,f_{\bar{l}}(\mathbf{x})e^{i\eta}\ , \tag{33}$$

where C is a real constant. By using the previous procedure, one can obtain the spectra also for all the other modes, provided that the functions $f_l(\mathbf{x})$ have the form

$$f_l(\mathbf{x}) = \sigma_l(\mathbf{x})e^{i[\psi(\mathbf{x})+\theta_l]}\ , \tag{34}$$

where $\sigma_l(\mathbf{x})$ is real, $\psi(\mathbf{x})$ does not depend on l, and θ_l does not depend on $\mathbf{x}$; this is true, for example, in the case of Gauss-Laguerre modes. Let us assume, furthermore, for definiteness that $\theta_{\bar{l}} = 0$. As a matter of fact, by using the available LOF, one can obtain the function $\Gamma(\mathbf{x},t;\mathbf{x}',0)$ with $\phi_L(\mathbf{x}) = \psi(\mathbf{x}) + \eta$. The spectrum of squeezing $S_l(\omega,\theta)$ can be obtained from the formula

$$S_l(\omega,\theta) = \int_{-\infty}^{\infty} dt\,e^{-i\omega t}\int d^2\mathbf{x} \times \int \mathrm{d}^2\mathbf{x}'\,\sigma_l(\mathbf{x})\sigma_l(\mathbf{x}')\Gamma(\mathbf{x},t;\mathbf{x}',0)\ , \tag{35}$$

where $\theta = \eta - \theta_l$.

Needless to say, all the previous considerations in this section can be extended to the Fourier transform

$$\tilde{\Gamma}(\mathbf{x},\mathbf{x}';\omega) = \int_{-\infty}^{\infty} dt\,e^{-i\omega t}\Gamma(\mathbf{x},t;\mathbf{x}',0)\ , \tag{36}$$

which is more easily determined experimentally.

The previous discussion showed that the spectrum of squeezing can be expressed in terms of the spatial correlation function; under appropriate conditions one can show that, conversely, the correlation function can be expressed in terms of the spectral functions $S_{l,l'}(\omega)$ defined in Eq. (20). Precisely, the conditions are that the function $\phi_L(\mathbf{x})$ in Eq. (26) is constant, i.e., $\phi_L(\mathbf{x}) = \phi_L$, hence $\psi(\mathbf{x}) = 0$ in Eq. (34). As a matter of fact, starting from Eqs. (36) and (28), inserting Eq. (26) and the expansion (16), and using Eq. (34), one can obtain

$$\tilde{\Gamma}(\mathbf{x},\mathbf{x}';\omega) = \sum_{l,l'}\sigma_l(\mathbf{x})\sigma_{l'}(\mathbf{x}')S_{l,l'}(\omega) \tag{37}$$

with ϕ_L replaced by $\phi_L - \theta_l$ in Eqs. (20) and (21).

In a more realistic description of detection the finite size of the detectors should be taken into account. In the case of an array of small detectors in the transverse plane, one is led to consider the operators

$$A_{H\mathbf{j}}(t) = \frac{1}{N_{\mathbf{j}}^{\frac{1}{2}}} \int_{\Omega_{\mathbf{j}}} d^2\mathbf{x}\, \alpha_L^*(\mathbf{x}) A(\mathbf{x},t) \,, \tag{38}$$

where the index $\mathbf{j} = (j_x, j_y)$ indicates the position of the detector $\mathbf{j}$ in the (x,y) plane, the integration is carried out over the area $\Omega_{\mathbf{j}}$ of the $\mathbf{j}$th detector, and $N_{\mathbf{j}} = \int_{\Omega_{\mathbf{j}}} d^2\mathbf{x}\, |\alpha_L(\mathbf{x})|^2$. Notice that with the definition (38) one has

$$\left[A_{H\mathbf{j}}(t), A_{H\mathbf{j}'}^\dagger(t)\right] = \delta_{\mathbf{j},\mathbf{j}'} \,. \tag{39}$$

From Eqs. (12) and (13a) we see that the spectrum of squeezing can be written as

$$S(\omega) = 2\gamma \frac{1}{N} \int_{-\infty}^{+\infty} dt\, e^{-i\omega t} \times \sum_{\mathbf{j},\mathbf{j}'} N_{\mathbf{j}}^{\frac{1}{2}} N_{\mathbf{j}'}^{\frac{1}{2}} \langle : \delta E_{H\mathbf{j}}(t)\, \delta E_{H\mathbf{j}'}(0) : \rangle \,, \tag{40}$$

where the homodyne field $\mathcal{E}_{H\mathbf{j}}$ is defined as

$$\mathcal{E}_{H\mathbf{j}}(t) = A_{H\mathbf{j}}^\dagger(t) + A_{H\mathbf{j}}(t) \,. \tag{41}$$

A correlation function between the homodyne field measured at the pixels $\mathbf{j}$ and $\mathbf{j}'$, similar to that defined by Eq. (28), can be introduced as

$$\Gamma_{\mathbf{j}\mathbf{j}'}(t) = 2\gamma \frac{1}{(\Omega_{\mathbf{j}}\Omega_{\mathbf{j}'})^{\frac{1}{2}}} \langle : \delta\mathcal{E}_{H\mathbf{j}}(t)\, \delta\mathcal{E}_{H\mathbf{j}'}(0) : \rangle \,. \tag{42}$$

If the LOF is a slowly varying function of the transverse coordinates, or the dimensions of the detectors are small enough that the function $\rho_L(\mathbf{x}) \approx \rho_{\mathbf{j}}$, constant over each region $\Omega_{\mathbf{j}}$, the expression (40) for the spectrum reduces to

$$S(\omega) = \frac{1}{N} \int_{-\infty}^{+\infty} dt\, e^{-i\omega t} \sum_{\mathbf{j},\mathbf{j}'} \Omega_{\mathbf{j}}\Omega_{\mathbf{j}'}\, \rho_{\mathbf{j}}\rho_{\mathbf{j}'}\, \Gamma_{\mathbf{j}\mathbf{j}'}(t) \,. \tag{43}$$

The quantities $\rho_{\mathbf{j}}\rho_{\mathbf{j}'}\Gamma_{\mathbf{j}\mathbf{j}'}$ are those which are actually measured in a realistic experiment. In the limit of small detector size one easily finds that

$$\Gamma_{\mathbf{j}\mathbf{j}'}(t) = \frac{1}{\Omega_{\mathbf{j}}\Omega_{\mathbf{j}'}} \int_{\Omega_{\mathbf{j}}} d^2\mathbf{x} \int_{\Omega_{\mathbf{j}'}} d^2\mathbf{x}'\, \Gamma(\mathbf{x},t;\mathbf{x}',0) \,. \tag{44}$$

Clearly, in the limit in which the pixel size becomes infinitesimal $\Gamma_{\mathbf{j}\mathbf{j}'}(t)$ converges to $\Gamma(\mathbf{x},t;\mathbf{x}',0)$, and Eq. (43) reduces to Eq. (27).

The finite size of detectors must also be kept in mind when one meets integrable divergences in the expression of the correlation function Γ.

We end this section with a simple remark. If instead of the normally ordered spectrum $S(\omega)$ one considers the spectrum $V(\omega)$ given by Eq. (7), which is linked to $S(\omega)$ by Eq. (9), the corresponding correlation function $\Gamma_V(\mathbf{x},t;\mathbf{x}',0)$ such that

$$V(\omega) = \int_{-\infty}^{\infty} dt\, e^{-i\omega t} \int d^2\mathbf{x} \int d^2\mathbf{x}'\, \frac{\rho_L(\mathbf{x})\rho_L(\mathbf{x}')}{N} \times \Gamma_V(\mathbf{x},t;\mathbf{x}',0) \,, \tag{45}$$

is given by

$$\Gamma_V(\mathbf{x},t;\mathbf{x}',0) = \Gamma(\mathbf{x},t;\mathbf{x}',0) + \delta(\mathbf{x}-\mathbf{x}')\delta(t) \,, \tag{46}$$

and the singular part in Eq. (46) corresponds to the shot noise contribution.

IV. THE SPECTRUM OF THE INTENSITY FLUCTUATIONS

Up to this point we have considered only the phase dependent spectrum of squeezing. In this section we analyze, instead, the spectrum of the intensity fluctuations, which can be detected by direct observation, and is given by [20]

$$V_I(\omega) = \int_{-\infty}^{\infty} dt\, e^{-i\omega t} \int d^2\mathbf{x} \times \int d^2\mathbf{x}'\, \langle \delta I_{out}(\mathbf{x},t)\, \delta I_{out}(\mathbf{x}',0) \rangle \,, \tag{47}$$

where

$$\delta I_{out}(\mathbf{x},t) = I_{out}(\mathbf{x},t) - \langle I_{out}(\mathbf{x},t) \rangle \,, \tag{48}$$

and

$$I_{out}(\mathbf{x},t) = A_{out}^\dagger(\mathbf{x},t) A_{out}(\mathbf{x},t) \tag{49}$$

is proportional to the intensity of the output field, as measured by a pointlike detector placed at the position $\mathbf{x}$ in the transverse plane just in front of the coupling mirror.

By using Eq. (1) one obtains, as usual,

$$V_I(\omega) = S_N \left[1 + S_I(\omega)\right] \tag{50}$$

where

$$S_N = \int d^2\mathbf{x}\, \langle I_{out}(\mathbf{x},0) \rangle \,, \tag{51}$$

and

$$S_I(\omega) = S_N^{-1} \int_{-\infty}^{\infty} dt\, e^{-i\omega t} \int d^2\mathbf{x} \times \int d^2\mathbf{x}'\, \langle : \delta I_{out}(\mathbf{x},t)\, \delta I_{out}(\mathbf{x}',0) : \rangle \,. \tag{52}$$

The first term in Eq. (50) represents the shot noise. Because of the normal and time ordering, by using Eq. (11) one has

$$S_I(\omega) = 4\gamma^2 S_N^{-1} \int_{-\infty}^{\infty} dt\, e^{-i\omega t} \int d^2\mathbf{x} \times \int d^2\mathbf{x}'\, \langle : \delta I(\mathbf{x},t)\, \delta I(\mathbf{x}',0) : \rangle \,, \tag{53}$$

where

$$I(\mathbf{x},t) = A^\dagger(\mathbf{x},t)A(\mathbf{x},t) \; ; \tag{54}$$

moreover, $S_N = 2\gamma N_I$, with

$$N_I = \int d^2\mathbf{x}\langle A^\dagger(\mathbf{x},0)A(\mathbf{x},0)\rangle .$$

Let us now assume that the steady-state mean value $\langle A(\mathbf{x},0)\rangle$ is much larger than the fluctuations of $A(\mathbf{x},t)$. In this case, if we set

$$A(\mathbf{x},t) = \langle A(\mathbf{x},0)\rangle + \delta A(\mathbf{x},t) \tag{55}$$

in Eq. (53) and we keep only the dominant terms, we obtain

$$S_I(\omega) = 2\gamma \int_{-\infty}^{\infty} dt\, e^{-i\omega t}\langle : \delta E_I(t)\, \delta E_I(0) : \rangle \; , \tag{56}$$

$$E_I = \frac{1}{N_I^{\frac{1}{2}}} \int d^2\mathbf{x}\, [\langle A(\mathbf{x},0)\rangle A^\dagger(\mathbf{x},t) + \langle A(\mathbf{x},0)\rangle^* A(\mathbf{x},t)] \; . \tag{57}$$

As one can see, Eqs. (56) and (57) are identical to Eqs. (12) and (13a), respectively, provided that $\alpha_L(\mathbf{x})$ is replaced by $\langle A(\mathbf{x},0)\rangle$ (which in turn implies the replacement of N by N_I and E_H by E_I). Hence in the direct detection of the intensity fluctuations the mean field $\langle A(\mathbf{x},0)\rangle$ plays the same role as the local oscillator $\alpha_L(\mathbf{x})$ in the homodyne detection scheme. All the formulas (18)–(26) hold also for the intensity spectrum $S_I(\omega)$, provided $\alpha_L(\mathbf{x})$ is replaced by $\langle A(\mathbf{x},0)\rangle$, ρ_L by ρ_I, and ϕ_L by ϕ_I, where

$$\langle A(\mathbf{x},0)\rangle = \rho_I(\mathbf{x}) e^{i\phi_I(\mathbf{x})} \; . \tag{58}$$

The same holds true for Eqs. (27) and (28) if one replaces Γ by

$$\Gamma_I(\mathbf{x},t;\mathbf{x}',0) = 2\gamma\langle : \delta\mathcal{E}_I(\mathbf{x},t)\, \delta\mathcal{E}_I(\mathbf{x}',0) : \rangle \; , \tag{59}$$

where

$$\mathcal{E}_I(\mathbf{x},t) = A(\mathbf{x},t)e^{-i\phi_I} + A(\mathbf{x},t)^\dagger e^{i\phi_I} \; . \tag{60}$$

It is easy to verify that, under the same hypothesis that the field fluctuations are small with respect to the mean field, Γ_I coincides with the normally ordered correlation function of the intensity fluctuations, defined as

$$\Gamma_2(\mathbf{x},t;\mathbf{x}',0) = 2\gamma \frac{\langle : \delta I(\mathbf{x},t)\, \delta I(\mathbf{x}',0) : \rangle}{[\langle I(\mathbf{x},0)\rangle \langle I(\mathbf{x}',0)\rangle]^{\frac{1}{2}}} \; . \tag{61}$$

At this point we have finished the general part of this paper. In the following we turn our attention to the special case of the optical parametric oscillator.

V. THE QUANTUM MODEL FOR THE OPO

The standard model for the degenerate OPO in a Fabry-Pérot cavity [21,22] is here generalized to include diffractive effects during the free propagation.

We consider a cavity with plane mirrors containing a nonlinear $\chi^{(2)}$ medium which converts a field of frequency $2\omega_s$ into a field of frequency ω_s and vice versa. A coherent, plane wave field of frequency $2\omega_s$ is injected into the cavity. Two longitudinal modes of the cavity, labeled by 0 and 1, are close to resonance with the fundamental frequency $2\omega_s$ and with the subharmonic frequency ω_s, respectively. We assume conditions such that only these two longitudinal cavity modes are relevant. Moreover, we assume the validity of the paraxial and slowly varying envelope approximation for both fields.

The interaction picture in which the frequency ω_s is eliminated for the signal field, and the frequency $2\omega_s$ is eliminated for the pump field, is adopted; $A_1(\mathbf{x},t)$ and $A_0(\mathbf{x},t)$ are the intracavity field envelope operators for signal and pump mode, respectively, which depend on the coordinate $\mathbf{x} = (x,y)$ of the point in the plane orthogonal to the optical axis z (Fig. 2).

In order to avoid difficulties arising from a continuum of transverse modes, we consider in the transverse plane (x,y) a square of side b and we assume periodic boundary conditions for the fields. A complete set of transverse modes of the resonator is then given by

$$f_{0,0}(\mathbf{x}) = \frac{1}{b} \; ,$$
$$f_{\mathbf{n}i}(\mathbf{x}) = \frac{\sqrt{2}}{b} \times \begin{cases} \cos(\mathbf{k_n}\cdot\mathbf{x}) & \text{for } i=1, \\ \sin(\mathbf{k_n}\cdot\mathbf{x}) & \text{for } i=2, \end{cases} \quad \mathbf{n} \neq (0,0) \; , \tag{62}$$

where $\mathbf{k_n} = \frac{2\pi\mathbf{n}}{b}$, $\mathbf{n} = (n_x, n_y)$, $n_x = 0,1,2,\ldots$, and $n_y = 0, \pm 1, \pm 2, \ldots$.

In the paraxial approximation, in which the transverse components of the wave vector are much smaller than the longitudinal component, the frequency of the transverse mode $\mathbf{n}$ is given by

$$\omega_{0,\mathbf{n}} = \omega_0 + \frac{c^2}{4\omega_s} k_{\mathbf{n}}^2 \; , \tag{63a}$$

$$\omega_{1,\mathbf{n}} = \omega_1 + \frac{c^2}{2\omega_s} k_{\mathbf{n}}^2 \; , \tag{63b}$$

where ω_0 and ω_1 are the frequencies of the axial mode $\mathbf{n} = (0,0)$ for the pump and signal fields, respectively.

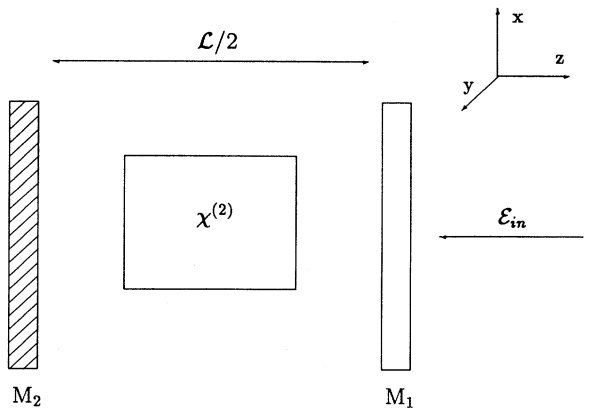

FIG. 2. Scheme of the cavity. The mirror M_1 has a high reflectivity, M_2 is completely reflecting. $\mathcal{E}_{in}$ is the input field of frequency $2\omega_s$.

The field envelope operators for the two fields can be expanded on the basis (62) as follows:

$$A_0(\mathbf{x}) = \sum_{i=1,2} \sum_{\mathbf{n}} f_{\mathbf{n}i}(\mathbf{x})\, b_{\mathbf{n}i} \ , \tag{64a}$$

$$A_1(\mathbf{x}) = \sum_{i=1,2} \sum_{\mathbf{n}} f_{\mathbf{n}i}(\mathbf{x})\, a_{\mathbf{n}i} \ , \tag{64b}$$

where the operators $a_{\mathbf{n}i}$ and $b_{\mathbf{n}i}$ obey the canonical commutation rules $[a_{\mathbf{n}i}, a^\dagger_{\mathbf{n}'i'}] = \delta_{\mathbf{n},\mathbf{n}'}\delta_{i,i'}$ and $[b_{\mathbf{n}i}, b^\dagger_{\mathbf{n}'i'}] = \delta_{\mathbf{n},\mathbf{n}'}\delta_{i,i'}$.

The model is formulated in terms of a master equation for the density operator of the multimode system:

$$\frac{d\rho}{dt} = \frac{1}{i\hbar}[H,\rho] + \sum_{\mathbf{n}i} \Lambda^0_{\mathbf{n}i}\,\rho + \sum_{\mathbf{n}i} \Lambda^1_{\mathbf{n}i}\,\rho \ . \tag{65}$$

The Liouvillian terms

$$\Lambda^0_{\mathbf{n}i} = \gamma_0 \left[2b_{\mathbf{n}i}\rho b^\dagger_{\mathbf{n}i} - \rho b^\dagger_{\mathbf{n}i} b_{\mathbf{n}i} - b^\dagger_{\mathbf{n}i} b_{\mathbf{n}i}\rho \right] \ , \tag{66a}$$

$$\Lambda^1_{\mathbf{n}i} = \gamma_1 \left[2a_{\mathbf{n}i}\rho a^\dagger_{\mathbf{n}i} - \rho a^\dagger_{\mathbf{n}i} a_{\mathbf{n}i} - a^\dagger_{\mathbf{n}i} a_{\mathbf{n}i}\rho \right] \tag{66b}$$

describe the damping of the mode $\mathbf{n}i$ for pump and signal field, respectively; γ_0 and γ_1 are the cavity damping rates of the two fields.

The system Hamiltonian which describes the coupled dynamics of signal and pump field is given by

$$H = H_{FREE} + H_{EXT} + H_{INT} \ . \tag{67}$$

Free propagation of the fields in the cavity is described by

$$H_{FREE} = \hbar \sum_{\mathbf{n}i} [(\omega_{1,\mathbf{n}} - \omega_s)\ a^\dagger_{\mathbf{n}i} a_{\mathbf{n}i} + (\omega_{0,\mathbf{n}} - 2\omega_s)\ b^\dagger_{\mathbf{n}i} b_{\mathbf{n}i}] \ . \tag{68}$$

Taking into account the field expansions (64a) and the k^2 dependence of the mode's eigenfrequencies (63a), the free Hamiltonian (68) can be recast as

$$H_{FREE} = \hbar \int_B d^2\mathbf{x}\, A^\dagger_1(\mathbf{x}) \left(\omega_1 - \omega_s - \frac{c^2}{2\omega_s}\nabla^2_\perp \right) A_1(\mathbf{x}) + \hbar \int_B d^2\mathbf{x}\, A^\dagger_0(\mathbf{x}) \left(\omega_0 - 2\omega_s - \frac{c^2}{4\omega_s}\nabla^2_\perp \right) \times A_0(\mathbf{x}) \ , \tag{69}$$

where the integration is performed over the transverse area $B = (-b/2, b/2) \times (-b/2, b/2)$. This shows the contribution of the transverse Laplacian

$$\nabla^2_\perp = \frac{\partial^2}{\partial x^2} + \frac{\partial^2}{\partial y^2} \tag{70}$$

which describes diffraction in the paraxial approximation.

The standard OPO interaction Hamiltonian is here generalized to the multitransverse mode case as

$$H_{INT} = \frac{i\hbar g}{2} \int_B d^2\mathbf{x} \left\{ A_0(\mathbf{x}) \left[A^\dagger_1(\mathbf{x}) \right]^2 - A^\dagger_0(\mathbf{x}) A^2_1(\mathbf{x}) \right\} \ , \tag{71}$$

where g is the coupling constant, proportional to the second-order susceptibility $\chi^{(2)}$. The interaction (71) will in general couple the dynamical evolution of all the transverse modes.

The external Hamiltonian is given by

$$H_{EXT} = i\hbar \int_B d^2\mathbf{x} \left[\mathcal{E}^*_{in} A_0(\mathbf{x}) - \mathcal{E}_{in} A^\dagger_0(\mathbf{x}) \right] = i\hbar \left[\mathcal{E}^*_{in} b_{0,0} - \mathcal{E}_{in} b^\dagger_{0,0} \right] \ , \tag{72}$$

where $\mathcal{E}_{in}$ is the amplitude of the input field.

VI. SEMICLASSICAL MODEL AND PATTERN FORMATION

The semiclassical model which corresponds to the quantum model introduced in the previous section is formulated in terms of dynamical equations for the c-number fields $\mathcal{A}_0(\mathbf{x}, t)$ and $\mathcal{A}_1(\mathbf{x}, t)$, proportional to the mean values of the field envelope operators $A_0(\mathbf{x}, t)$ and $A_1(\mathbf{x}, t)$.

$$\frac{\partial}{\partial t}\mathcal{A}_0 = \gamma_0 \left[-(1 + i\Delta_0)\mathcal{A}_0 + E - \mathcal{A}^2_1 + i\frac{c^2}{4\omega_s\gamma_0}\nabla^2_\perp \mathcal{A}_0 \right] \ , \tag{73a}$$

$$\frac{\partial}{\partial t}\mathcal{A}_1 = \gamma_1 \left[-(1 + i\Delta_1)\mathcal{A}_1 + \mathcal{A}^*_1 \mathcal{A}_0 + i\frac{c^2}{2\omega_s\gamma_1}\nabla^2_\perp \mathcal{A}_1 \right] \ . \tag{73b}$$

Here the normalized variables are defined as in Ref. [25],

$$\mathcal{A}_0 = \frac{g}{\gamma_1}\langle A_0 \rangle \ , \qquad \mathcal{A}_1 = \frac{g}{\sqrt{2\gamma_0\gamma_1}}\langle A_1 \rangle \ ; \tag{74}$$

the parameter $E = (g/\gamma_1)\,\mathcal{E}_{in}$ is proportional to the amplitude of the input field, and

$$\Delta_0 = \frac{\omega_0 - 2\omega_s}{\gamma_0} \ , \tag{75}$$

$$\Delta_1 = \frac{\omega_1 - \omega_s}{\gamma_1} \tag{76}$$

are the detuning parameters for the pump and signal fields, respectively.

The OPO below threshold is characterized by the uniform stationary state

$$\mathcal{A}_{0s} = \frac{E(1 - i\Delta_0)}{1 + \Delta^2_0}, \quad \mathcal{A}_{1s} = 0 \ . \tag{77}$$

The linear stability analysis of this solution, performed in the "continuum" limit $b \to \infty$, shows that the threshold for signal generation depends crucially on the sign of the detuning parameter Δ_1 [23] as follows.

(a) When $\Delta_1 > 0$ the trivial solution (77) becomes unstable with respect to the onset of a uniform signal

wave propagating along the longitudinal axis, and, defining $I_{0s} = |\mathcal{A}_{0s}^2|$, the threshold for signal generation is $I_{0s}^{(thr)} = 1 + \Delta_1^2$.

(b) when $\Delta_1 < 0$ the instability generates signal waves in two symmetrical off-axial directions; the critical transverse wave vector which characterizes these waves is $k_c = \sqrt{-\Delta_1 2\omega_s\gamma_1/c^2}$. The instability threshold is $I_{0s}^{(thr)} = 1$; hence lower then in the previous case.

These results can be better understood if one considers a signal field of the form

$$\mathcal{A}_1 \propto e^{i\mathbf{k}\cdot\mathbf{x}}, \qquad \mathbf{x} = (x, y), \qquad \mathbf{k} = (k_x, k_y), \tag{78}$$

which represents a tilted plane wave that propagates at angle $k/k_z = \left(k_x^2 + k_y^2\right)^{\frac{1}{2}}/k_z$, where $k_z = \omega_s/c$ with respect to the optical axis. By inserting Eq. (78) into Eq. (73b), one finds that the detuning parameter of mode $\mathbf{k}$ is given by

$$\Delta_k = \Delta_1 + (c^2/2\omega_s\gamma_1)k^2, \tag{79}$$

where the second contribution arises from the transverse Laplacian. Hence, when $\Delta_1 \geq 0$, the axial mode $\mathbf{k} = (0, 0)$ is closest to resonance with the frequency of the signal field, and hence has the maximum gain, which leads to the emission of a uniform signal wave traveling along the longitudinal axis.

On the other hand, when Δ_1 is negative, the detuning Δ_k vanishes for

$$k = k_c = \sqrt{-\Delta_1 2\omega_s\gamma_1/c^2}\,; \tag{80}$$

this resonance condition characterizes, in this case, the critical modes, which have the largest gain. These modes form a cone around the longitudinal axis. However, the process of parametric down conversion leads to the emission of photon pairs with conservation of the transverse photon momentum, and the system breaks the rotational symmetry by emitting two signal waves in two symmetrical directions.

It must be observed, in this connection, that the model assumes equal refractive indices for the pump and the signal fields so that, in the absence of the cavity, the emission of the signal photons would occur in the axial direction. However, due to the resonance mechanism described above, the cavity is able to force the system to violate slightly the phase matching conditions, emitting the signal photons at a small angle with respect to the longitudinal axis. This violation is admissible, because the phase mismatch accumulated during the passage of the radiation through the crystal is very small, as is assumed by the conditions of validity of the mean field (i.e., single longitudinal mode) model used here. By taking into account that $\gamma_1 = ct_1^2/2\mathcal{L}$, where $\mathcal{L}$ is the cavity round trip length and t_1 is the transmittivity coefficient of the input-output mirror at frequency ω_s, one has that the angle of emission is given by

$$\frac{k_c}{k_z} = \left(\frac{-\Delta_1}{2\pi}\frac{\lambda_s}{\mathcal{L}}t_1^2\right)^{\frac{1}{2}}, \tag{81}$$

where $\lambda_s = 2\pi/k_z$ is the wavelength of the signal field.

In conclusion, for $\Delta_1 < 0$, when the input intensity E^2 overcomes the threshold value $E^2 = 1 + \Delta_0^2$, one has the emission of a signal field of the form

$$\begin{aligned} A_1(x) &= \sigma e^{i\phi_+} e^{ik_c x} + \sigma e^{i\phi_-} e^{-ik_c x} \\ &= \sigma\cos\left(k_c x + \frac{\phi_+ - \phi_-}{2}\right), \end{aligned} \tag{82}$$

where the amplitude σ is equal for the two signal waves, and we have taken into account that $\phi_+ + \phi_- = 0$ [14]. The configuration (82) corresponds to a stripe pattern, similar to the rolls of the Bénard instability in fluids [19,26]. Thus, for $\Delta_1 < 0$, when the OPO overcomes threshold, it breaks simultaneously the translational and the rotational symmetry. In Eq. (82) we have assumed that the rolls are orthogonal to the x axis in the transverse plane. The phase difference $\phi_+ - \phi_-$ is arbitrary, which means that the roll pattern has an arbitrary position in the transverse plane.

When the input intensity E^2 is increased enough above threshold, one meets the appearance of zigzag patterns and complex dynamical patterns, as described in [23].

VII. THE ANGULAR DEPENDENCE OF SQUEEZING

In Sec. II we said that, in order to describe the spatial structure of squeezed states, one must probe the squeezed field using various local oscillator fields, corresponding to the functions of an orthonormal set in the transverse plane. We illustrate now that the orthonormal set (62) is appropriate to describe the angular dependence of squeezing.

Clearly, the modes (62) correspond to a field configuration formed by the superposition of two tilted plane waves $\exp(i\mathbf{k}\cdot\mathbf{x})$ and $\exp(-i\mathbf{k}\cdot\mathbf{x})$. Note that, with respect to the general case of Eq. (34), the case of the orthonormal set (62) corresponds to $\psi(\mathbf{x}) = 0$ and $\theta_{\mathbf{n},i} = 0$; furthermore, for a local oscillator of the form $\alpha_L(\mathbf{x}) \propto f_{\mathbf{n}i}(\mathbf{x})\exp(\theta)$ the phase ϕ_L in Eq. (24) is independent of $\mathbf{x}$. We also observe that the choice of the orthonormal set (62) is appropriate for the analysis of the spatial structure of squeezed states, because squeezing is linked to the presence of pairs of twin photons, and, as occurs in the case of the OPO, it is reasonable that the two photons are associated with two tilted plane waves with transverse wave vectors $\mathbf{k}$ and $-\mathbf{k}$.

Now, let us consider the spatial spectrum of squeezing $S_{\mathbf{n}i}(\omega, \theta)$ and let us assume that, as in the case we will examine below, it does not depend on the index i. The functions $S_{\mathbf{n}}(\omega, \theta)$ will therefore describe how the level of squeezing varies with the angle $\mathbf{k}_{\mathbf{n}}/k_z$ with respect to the longitudinal axis. In particular, for $\mathbf{n} = (0, 0)$, $S_{(0,0)}(\omega, \theta)$ describes the level of squeezing in the longitudinal direction, which is the only one described by plane wave theories.

VIII. THE OPO BELOW THRESHOLD: SPECTRUM OF QUANTUM FLUCTUATIONS

We now turn to consider the OPO below the threshold for signal generation, in the approximation in which the complete quantum model (including both signal and pump fields) is linearized around the semiclassical stationary solution (77). In this case, the complete model of Sec. V reduces to a simpler quantum model which involves only the signal field, while the pump field appears only as a classical quantity equal to the stationary semiclassical value. In this way, pump depletion is neglected. The model is identical to that of Ref. [16], and it is formulated in terms of a master equation for the density operator of the multimode system. The interaction Hamiltonian (71) reduces to

$$H_{INT} = i\hbar\gamma_1 \frac{\mathcal{A}_{0s}}{2} \int_B d^2\mathbf{x} \left\{ \left[A_1^\dagger(\mathbf{x})\right]^2 - A_1^2(\mathbf{x}) \right\} = i\hbar\gamma_1 \frac{\mathcal{A}_{0s}}{2} \sum_{i=1,2} \sum_{\mathbf{n}} \left[\left(a_{\mathbf{n}i}^\dagger\right)^2 - a_{\mathbf{n}i}^2 \right] , \quad (83)$$

where $\mathcal{A}_{0s}$ is proportional to the amplitude of the plane wave pump field E, according to Eq. (77), and for the sake of simplicity we assume that $\mathcal{A}_{0s}$ is real and positive. Thus the model in this case describes the dynamics of infinite, independent, single-mode degenerate OPO's.

The quantum properties of the near field can be expressed in terms of the spectra of quantum fluctuations of the single-mode OPO's, defined as

$$S_{\mathbf{n}i}(\omega) = 2\gamma_1 \int_{-\infty}^{\infty} dt\, e^{-i\omega t} \langle : \delta A_{\mathbf{n}i}(t)\, \delta A_{\mathbf{n}i}(0) : \rangle , \quad (84a)$$

$$A_{\mathbf{n}i}(t) = a_{\mathbf{n}i}^\dagger(t)\, e^{i\phi_{\mathbf{n}i}} + a_{\mathbf{n}i}(t) e^{-i\phi_{\mathbf{n}i}} . \quad (84b)$$

By indicating $\overline{\omega} = \omega/\gamma_1$, these spectra read [27]

$$S_{\mathbf{n}i}(\overline{\omega}) = 4\mathcal{A}_{0s} \left[\left(1 + \Delta_k^2 - \mathcal{A}_{0s}^2 - \overline{\omega}^2\right)^2 + 4\overline{\omega}^2 \right]^{-1} \times \{ 2\mathcal{A}_{0s} + + \mathrm{Re}[\left(1 + \overline{\omega}^2 - \Delta_k^2 + \mathcal{A}_{0s}^2 - 2i\Delta_k\right) \times \exp(-2i\phi_{\mathbf{n}i})] \} , \quad (85)$$

where Δ_k is the detuning of modes with $|\mathbf{k_n}| = k$, given by Eq. (79). For the quadrature component $i(a_{\mathbf{n}i}^\dagger - a_{\mathbf{n}i})$, when $\Delta_1 \leq 0$, complete suppression of quantum noise at zero frequency is predicted at threshold for the critical modes, i.e., for $k = \sqrt{-\Delta_1 2\omega_s\gamma_1/c^2}$ [16]. Of course, at threshold or very near threshold the linear model (83) is no longer valid; however, this result must be viewed as an asymptotic ideal limit of the behavior of the OPO below threshold.

The expression of the spectrum of squeezing for a generic LOF is given by Eq. (23) together with Eqs. (19)–(22), with l replaced by $\mathbf{n}i$. Note that $S_{\mathbf{n}i}$ depends on the index i only via the phase $\phi_{\mathbf{n}i}$.

Following Eq. (35), the single-mode spectrum $S_{\mathbf{n}i}$ is given by

$$S_{\mathbf{n}i}(\omega) = \int_{-\infty}^{\infty} dt\, e^{-i\omega t} \int_B d^2\mathbf{x} \times \int_B d^2\mathbf{x}'\, f_{\mathbf{n}i}(\mathbf{x}) f_{\mathbf{n}i}(\mathbf{x}') \Gamma(\mathbf{x}, t; \mathbf{x}', 0) , \quad (86)$$

where the phase $\phi_L(\mathbf{x})$ in the definition (28) and (26) of the correlation function Γ must be taken equal to $\phi_{\mathbf{n}i}$.

In the following, for the sake of simplicity, we assume that the LOF used to measure the spatial correlation function $\Gamma(\mathbf{x}, t; \mathbf{x}', 0)$ has a phase ϕ_L which is constant over the transverse plane. Hence all the phases $\phi_{\mathbf{n}i}$ given by Eq. (19) (with l replaced by $\mathbf{n}i$) are equal to ϕ_L, and the function $S_{\mathbf{n}i}$ does not depend on the index i, which therefore will be dropped in the following.

Taking into account the translational symmetry of the OPO below threshold, it turns out that the two-point correlation function Γ depends only the distance $(\mathbf{x} - \mathbf{x}')$ and the spectrum is just the spatiotemporal Fourier transform of the correlation function:

$$S_{\mathbf{n}}(\omega) = \int_{-\infty}^{\infty} dt\, e^{-i\omega t} \times \int_B d^2\mathbf{x} \cos\left[\mathbf{k_n} \cdot (\mathbf{x} - \mathbf{x}')\right] \Gamma(\mathbf{x} - \mathbf{x}', t) . \quad (87)$$

Clearly there exists the inverse relation of Eq. (87):

$$\Gamma(\mathbf{x} - \mathbf{x}', t) = \int_{-\infty}^{+\infty} \frac{d\omega}{2\pi} e^{i\omega t} \left\{ \frac{S_{0,0}}{b^2} + \sum_{\mathbf{n}\neq(0,0)} \frac{2}{b^2} \times \cos\left[\mathbf{k_n} \cdot (\mathbf{x} - \mathbf{x}')\right] S_{\mathbf{n}}(\omega) \right\} , \quad (88)$$

Hence, the spatial spectrum of squeezing $S_{\mathbf{n}}(\omega)$ and the space-time correlation function are essentially the Fourier transform of each other, similarly to what one has in the theory developed in [10]. This is no longer true for different orthonormal sets, e.g., for Gauss-Laguerre modes. By using Eq. (88), from the spectra $S_{\mathbf{n}}(\omega)$, one can calculate the correlation function (28), which provides a deeper insight into the spatiotemporal behavior of a field, like that of the OPO below threshold, which is purely generated by quantum noise.

If one considers a set of pixels with finite size, the spatial correlation function $\Gamma_{\mathbf{j}\mathbf{j}'}(t)$ given by Eq. (42) becomes

$$\Gamma_{\mathbf{j}\mathbf{j}'}(t) = \int_{-\infty}^{+\infty} \frac{d\omega}{2\pi} e^{i\omega t} \left\{ \frac{S_{0,0}}{b^2} + \sum_{\mathbf{n}\neq(0,0)} \frac{2}{b^2} \mathrm{sinc}^2\left(\frac{k_{n_x} d_x}{2}\right) \mathrm{sinc}^2\left(\frac{k_{n_y} d_y}{2}\right) \times \cos\left[\mathbf{k_n} \cdot (\mathbf{x_j} - \mathbf{x_{j'}})\right] S_{\mathbf{n}}(\omega) \right\} , \quad (89)$$

where d_x and d_y are the transverse dimensions of the pixels (which are here assumed to be rectangular), $\mathrm{sinc}\, z = \sin z/z$, and $\mathbf{x_j}$ is the coordinate of the center of the $\mathbf{j}$th pixel. Provided that the dimensions of the detectors are small enough, compared to the minimum wave-

length $\lambda_{\mathbf{n}} = 2\pi/|\mathbf{k_n}|$ for which $S_{\mathbf{n}}$ is appreciably nonzero, Eq. (89) reduces to the previous expression (88), and $\Gamma_{\mathbf{jj'}}(t) \longrightarrow \Gamma(\mathbf{x_j} - \mathbf{x_{j'}}, t)$.

IX. TEMPORAL DYNAMICS OF FLUCTUATIONS

In order to simplify notation, here and in the following we shall consider the scaled variables

$$\begin{aligned} &\mathbf{r} = (\mathbf{x} - \mathbf{x}')/L_1 , && \mathbf{q} = L_1\mathbf{k} , \\ &\overline{\omega} = \omega/\gamma_1 , && \tau = \gamma_1 t , \end{aligned} \tag{90}$$

and a dimensionless version of the correlation function Γ defined by Eq. (28),

$$C(\mathbf{r},\tau) = \frac{L_1^2}{\gamma_1}\Gamma(\mathbf{r},\tau) , \tag{91}$$

where

$$L_1 = \left(\frac{c^2}{2\omega_s\gamma_1}\right)^{\frac{1}{2}} = \left(\frac{\lambda_s\mathcal{L}}{2\pi t_1^2}\right)^{\frac{1}{2}} \tag{92}$$

is the characteristic length of diffraction in a cavity. Moreover, we shall take the "continuum" limit $b \to \infty$ of Eq. (88), which is then replaced by

$$C(\mathbf{r},\tau) = \int_{-\infty}^{+\infty}\frac{d\overline{\omega}}{2\pi}e^{i\overline{\omega}\tau}\int\frac{d^2\mathbf{q}}{(2\pi)^2}\cos(\mathbf{q}\cdot\mathbf{r})S(q,\overline{\omega}) , \tag{93}$$

where $S(q,\overline{\omega})$ is still given by Eq. (85), with $(c^2/2\omega_s\gamma_1)^{\frac{1}{2}}\mathbf{k_n}$ replaced by $\mathbf{q}$. Note that S depends only on the modulus of the wave vector $\mathbf{q}$.

As a first step we have carried out the integration over the frequencies $\overline{\omega}$, which gives

$$S(q,\tau) \equiv \int_{-\infty}^{+\infty}\frac{d\overline{\omega}}{2\pi}e^{i\overline{\omega}\tau}S(q,\overline{\omega}) \tag{94}$$

$$= \begin{cases} e^{-\tau}\left\{\left(\mathcal{A}_{0s}^2 - \Delta_q^2\right)^{-\frac{1}{2}}\sinh\left[\left(\mathcal{A}_{0s}^2 - \Delta_q^2\right)^{\frac{1}{2}}\tau\right]\left[S_0(q) - 2\mathcal{A}_{0s}\cos 2\phi_L\right]\right. \\ \quad \left. +\cosh\left[\left(\mathcal{A}_{0s}^2 - \Delta_q^2\right)^{\frac{1}{2}}\tau\right]S_0(q)\right\} \text{ for } \mathcal{A}_{0s}^2 > \Delta_q^2 \\ e^{-\tau}\left\{\left(\Delta_q^2 - \mathcal{A}_{0s}^2\right)^{-\frac{1}{2}}\sin\left[\left(\Delta_q^2 - \mathcal{A}_{0s}^2\right)^{\frac{1}{2}}\tau\right]\left[S_0(q) - 2\mathcal{A}_{0s}\cos 2\phi_L\right]\right. \\ \quad \left. +\cos\left[\left(\Delta_q^2 - \mathcal{A}_{0s}^2\right)^{\frac{1}{2}}\tau\right]S_0(q)\right\} \text{ for } \Delta_q^2 > \mathcal{A}_{0s}^2 , \end{cases} \tag{95}$$

where

$$\begin{aligned} S_0(q) &= S(q,\tau=0) \\ &= 2\mathcal{A}_{0s}\frac{\mathcal{A}_{0s} + \cos 2\phi_L - \Delta_q\sin 2\phi_L}{1 - \mathcal{A}_{0s}^2 + \Delta_q^2} . \end{aligned} \tag{96}$$

This function evidences the well known phenomenon of critical slowing down of fluctuations. By defining a parameter ϵ which measures the distance from threshold

$$\epsilon^2 = I_{0s}^{(thr)} - I_{0s} = \begin{cases} 1 - \mathcal{A}_{0s}^2 , & \Delta_1 \le 0 \\ 1 + \Delta_1^2 - \mathcal{A}_{0s}^2 , & \Delta_1 > 0 , \end{cases} \tag{97}$$

we can write the long time behavior of the fluctuations of the critical modes as

$$\begin{aligned} S_(q_c,\tau) \approx &\left[S_0(q_c)\left(1 + \mathcal{A}_{0s}\right) - 2\mathcal{A}_{0s}\cos 2\phi_L\right] \\ &\times \exp\left(-\frac{\epsilon^2}{1 + \mathcal{A}_{0s}}\tau\right) , \end{aligned} \tag{98}$$

where $q_c = \sqrt{-\Delta_1}$ for $\Delta_1 \le 0$ [see Eqs. (80), (90), and (92)], and $q_c = 0$ for $\Delta_1 > 0$. Hence the fluctuations arising in the critical modes die out over a long time scale, and the relaxation time diverges approaching the threshold as $\approx (I_{0s}^{(thr)} - I_{0s})^{-1}$.

We would like to remark that the quantity $S_0(q)$, given by Eq. (96), is linked to the variance of the single-mode quadrature operator for the intracavity field. As follows from Eqs. (84b) and (94),

$$S_0(q) = 2\langle :\left(\delta A_{\mathbf{q}i}\right)^2: \rangle , \qquad i = 1,2 , \quad q = |\mathbf{q}| , \tag{99a}$$

$$A_{\mathbf{q}i} = a_{\mathbf{q}i}e^{-i\phi_L} + a_{\mathbf{q}i}^{\dagger}e^{i\phi_L} ; \tag{99b}$$

i.e., if we consider the discrete basis of transverse modes (62), $1 + \frac{1}{2}S_0(q)$ gives the variance of the single-mode operators $A_{\mathbf{q}i}$. Figures 3(a) and 3(b) plot $S_0(q)$, for $\phi_L = \pi/2$ and $\Delta_1 = 0$ and -1, respectively. For the $\phi_L = \pi/2$ field quadrature component, the level of quantum noise is reduced below shot noise for a band of wave vectors around the critical wave vector q_c. For this choice of the parameters Eq. (96) can be recast as

$$S_0(q) = -\frac{2\mathcal{A}_{0s}}{1 + \mathcal{A}_{0s}}\frac{\epsilon^2}{\epsilon^2 + (q^2 - q_c^2)^2} , \tag{100}$$

and it can be noted that the bandwidth of wave vectors for which there is significant quantum noise reduction be-

comes narrower and narrower as the threshold for signal generation is approached.

X. SPATIAL DYNAMICS OF FLUCTUATIONS

In this section we shall give some results about the equal-time spatial correlation function $C(\mathbf{r}, \tau = 0)$. We shall analyze separately the cases $\Delta_1 < 0$, $\Delta_1 = 0$, and $\Delta_1 > 0$.

A. Case $\Delta_1 < 0$

The threshold for signal generation is $\mathcal{A}_{0s} = 1$; the instability arises at threshold in the modes with $q = q_c = \sqrt{-\Delta_1}$, and the signal field above threshold is a stripe pattern. By performing the spatial integration in Eq. (93), and taking into account Eq. (96), the equal-time correlation function below threshold can be expressed in terms of the modified Bessel function of zero order K_0 [28] as

$$C(\mathbf{r}, \tau = 0) = \frac{2}{\pi}\left[\frac{\mathcal{A}_{0s}(\mathcal{A}_{0s} + \cos 2\phi_L)}{\epsilon}\mathrm{Im}K_0(zr) - \mathcal{A}_{0s}\sin 2\phi_L \mathrm{Re}K_0(zr)\right], \tag{101}$$

where

$$z = -i\sqrt{(q_c^2 + i\epsilon)} \overset{\epsilon \ll q_c}{\sim} -iq_c + \frac{\epsilon}{2q_c}, \tag{102}$$

and ϵ is defined by Eq. (97).

We now focus on the cases $\phi_L = 0$ or $\phi_L = \pi/2$, which correspond to the quadrature components of the field $A^\dagger + A$ and $i(A^\dagger - A)$, respectively. The large distance behavior of the spatial correlation can be described as

$$\lim_{q_c r \to \infty} C(r, \tau = 0) = C(0,0)\sqrt{\frac{2}{\pi r q_c}} e^{-\frac{\epsilon}{2q_c} r} \sin\left(q_c r + \frac{\pi}{4}\right) \times \left[1 + O\left(\frac{1}{q_c r}\right)\right], \tag{103}$$

where $C(0,0)$ is the value of the function at $r = 0$.

Two points are worth noting.

(1) As the system gets closer to threshold, the field becomes correlated over larger and larger spatial distances; Eq. (103) defines a correlation length $\xi = 2q_c/\epsilon$ which diverges approaching the threshold with a power law $\xi \approx (I_{0s}^{(thr)} - I_{0s})^{-\frac{1}{2}}$. This behavior is standard in equilibrium phase transitions, and it is also known in classical nonequilibrium systems [26]; here it is predicted for an optical system and for a quantum system far from equilibrium.

This effect is shown in Figs. 4(a) and 4(b), which plot the correlation function (101) for (a) $\mathcal{A}_{0s} = 0.99$, and (b) at threshold $\mathcal{A}_{0s} = 1$; one has $\Delta_1 = -1$ in both figures.

(2) The spatial correlation function shows a modulation with a wavelength $2\pi/k_c$ identical to that of the stripe pattern which appears above the OPO threshold; hence the onset of a spatial structure is heralded by the behavior of the correlation function. Other examples of fields generated by quantum noise are well known (e.g., the case of the laser below threshold), but our results show the existence of a quantum noise-generated field which exhibits an ordered spatial structure. We call it a *quantum image* [15,24], since the intensity distribution is constant over the transverse plane (the stationary state is homogeneous in space below threshold) and the modulation appears in the space correlation function.

So far we have shown phenomenena which have a classical counterpart; one could wonder which features of this correlation function show manifestly the quantum nature of the noise. The small distance behavior of the spatial correlation function can be seen to be

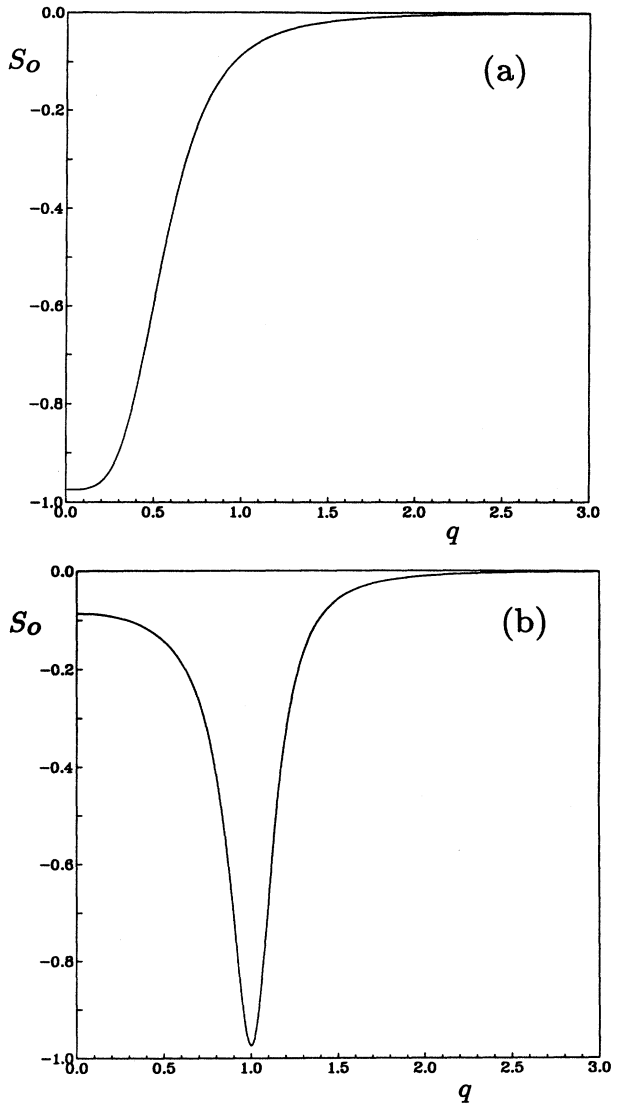

FIG. 3. Plot of $S(q, \tau = 0)$ [see Eq. (96)], which describes the level of quantum noise in mode q. Here $\phi_L = \pi/2$, $\mathcal{A}_{0s} = 0.95$, and (a) $\Delta_1 = 0$, (b) $\Delta_1 = -1$.

$$\lim_{q_c r \to 0} C(r, \tau = 0) = \begin{cases} -\frac{\mathcal{A}_{0s}\epsilon}{1+\mathcal{A}_{0s}} & \text{for } \phi_L = \frac{\pi}{2} \quad (104) \\ \frac{\mathcal{A}_{0s}(\mathcal{A}_{0s}+1)}{\epsilon} & \text{for } \phi_L = 0 \, . \quad (105) \end{cases}$$

The quantity $C(r = 0, \tau = 0) = \langle : [\delta \mathcal{E}_H(\mathbf{x}, t)]^2 : \rangle$ describes the normally ordered fluctuations of the homodyne field (26); Eq. (104) shows that for the quadrature field component $\phi_L = \pi/2$ this quantity is negative at finite distance ϵ from threshold, a circumstance which is clearly linked to the squeezing property of this field quadrature; in fact, as one has from Eq. (93),

$$C(r = 0, \tau = 0) = \int_{-\infty}^{+\infty} \frac{d\overline{\omega}}{2\pi} \int \frac{d^2\mathbf{q}}{(2\pi)^2} \, S(q, \overline{\omega}) \, , \quad (106)$$

and the fact that $S(q, \overline{\omega}) < 0$ is a signature of nonclassicity. This effect tends to disappear while approaching the threshold, because of the narrowing of the bandwidth of wave vectors for which there is quantum noise reduction below shot noise in the function $S_0(q)$ [see Eqs. (96) and (100) and Fig. 3]. Figure 5 plots the equal-time spatial correlation as a function of the scaled distance r for $\phi_L = \pi/2$ and $\Delta_1 = -1$.

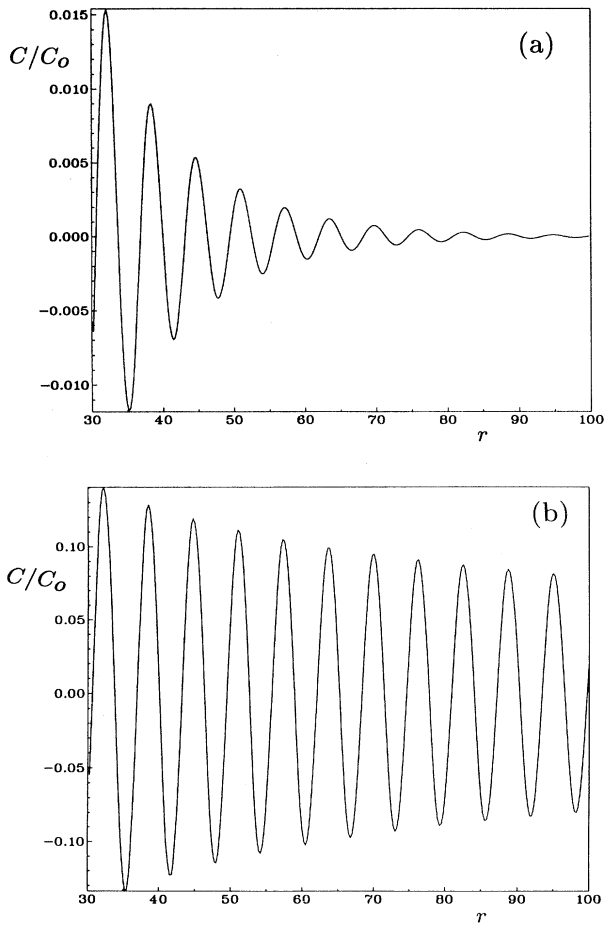

FIG. 4. The ratio $C(r, \tau = 0)/C(0, 0)$ is plotted at large distance r, for $\phi_L = \pi/2$ or $\phi_L = 0$. (a) $\mathcal{A}_{0s} = 0.99$ and the function is exponentially damped; (b) at threshold $\mathcal{A}_{0s} = 1$ the exponential damping vanishes because the correlation length diverges. In both figures $\Delta_1 = -1$ and the modulation is identical to that of the stripe pattern which appears above threshold.

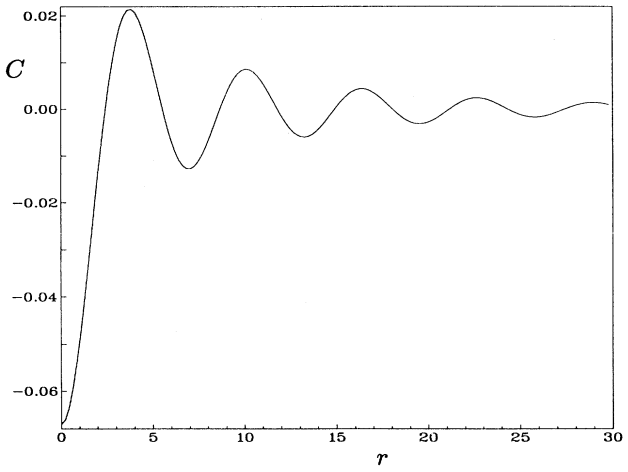

FIG. 5. Equal-time spatial correlation as a function of the scaled distance r, for $\Delta_1 = -1$ and $\phi_L = \pi/2$. The function has a space modulation and is negative at small distances. Here $\mathcal{A}_{0s} = 0.99$.

Normally ordered critical fluctuations of the orthogonal field component $\phi_L = 0$ are of course enhanced and $C(0, 0)$ diverges approaching the threshold as $(I_{0s}^{(thr)} - I_{0s})^{-\frac{1}{2}}$ [see Eq. (105)].

B. Case $\Delta_1 = 0$

The spatial correlation function is still given by Eq. (101), but the argument of the Bessel function is now $z_0 r$, with

$$z_0 = \sqrt{\epsilon} \exp\left(i\frac{\pi}{4}\right) . \quad (107)$$

Hence in this case the spatial correlation function depends only on r/ξ, where the correlation length is given by

$$\xi = \sqrt{\frac{2}{\epsilon}} = \sqrt{2}\left(I_{0s}^{(thr)} - I_{0s}\right)^{-\frac{1}{4}} . \quad (108)$$

When $\phi_L = 0$ or $\phi_L = \pi/2$, for example, the asymptotic behavior of the function at large distance can be written as

$$\lim_{r/\xi \to \infty} C(r, \tau = 0)$$

$$= 2C(0, 0)\sqrt{\frac{2}{\pi r/\xi}} \, e^{-r/\xi} \sin\left(r/\xi + \frac{\pi}{4}\right) , \quad (109)$$

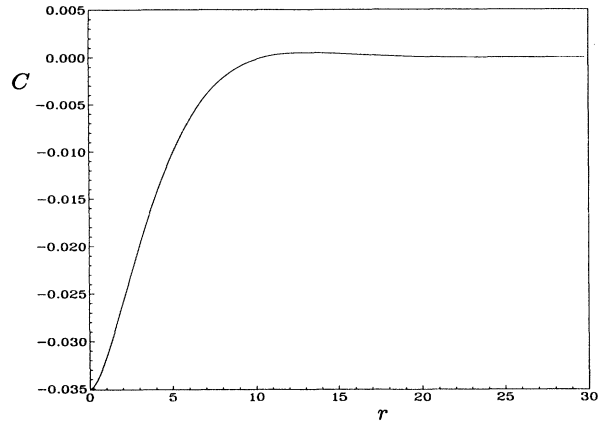

FIG. 6. Equal-time spatial correlation function for $\phi_L = \pi/2$ and $\Delta_1 = 0$. The spatial modulation of the correlation function has almost disappeared, and the function reproduces the spatial structure of the plane wave field which emerges above threshold. Here $\mathcal{A}_{0s} = 0.99$.

$$C(0,0) = \begin{cases} -\frac{\epsilon \mathcal{A}_{0s}}{2(1+\mathcal{A}_{0s})} & \text{for } \phi_L = \frac{\pi}{2} \\ \frac{\mathcal{A}_{0s}(1+\mathcal{A}_{0s})}{2\epsilon} & \text{for } \phi_L = 0. \end{cases} \quad (110)$$

The spatial correlation not only is slowly damped, as in the $\Delta_1 < 0$ case, but has also a slower and slower modulation as threshold is approached; also in this case the radial dependence of the correlation function reproduces the spatial structure of the signal field, which emerges from this instability, and is constant over the transverse plane.

Figure 6 shows an example of this correlation function for the field quadrature $\phi_L = \pi/2$. As in the previous case the fact that for $\phi_L = \pi/2$ $C(0,0)$ is negative is linked to the quantum noise reduction for a bandwidth of wave vectors around $q_c = 0$ [Fig. 3(b)].

C. Case $\Delta_1 > 0$

In this case the threshold for signal generation is $\mathcal{A}_{0s}^2 = 1 + \Delta_1^2$, and the field above threshold is constant over the transverse plane. The equal-time correlation function turns out to be given by

$$C(r, \tau = 0)$$

$$= \frac{\mathcal{A}_{0s}}{\pi} \left\{ \frac{\mathcal{A}_{0s} + \cos 2\phi_L}{\sqrt{\mathcal{A}_{0s}^2 - 1}} \left[K_0(r/\xi_1) - K_0(r/\xi_2) \right] - \mathcal{A}_{0s} \sin 2\phi_L \left[K_0(r/\xi_1) + K_0(r/\xi_2) \right] \right\}, \quad (111)$$

where

$$\xi_1 = \left(\Delta_1 - \sqrt{\Delta_1^2 - \epsilon^2} \right)^{-\frac{1}{2}} \underset{\epsilon \ll \Delta_1}{\sim} \frac{\sqrt{2\Delta_1}}{\epsilon}, \quad (112)$$

$$\xi_2 = \left(\Delta_1 + \sqrt{\Delta_1^2 - \epsilon^2} \right)^{-\frac{1}{2}} \underset{\epsilon \ll \Delta_1}{\sim} \frac{1}{\sqrt{2\Delta_1}}. \quad (113)$$

It can be easily seen that, as expected, this function has no spatial oscillation at all and the long range part of this correlation function has an exponential behavior at large distances:

$$\lim_{r/\xi_1 \to \infty} C(r, \tau = 0) \sim \frac{e^{-r/\xi_1}}{\sqrt{\pi r/\xi_1}}. \quad (114)$$

As in the case $\Delta_1 < 0$, the correlation length diverges approaching the threshold as $(I_{0s}^{(thr)} - I_{0s})^{-\frac{1}{2}}$.

At $r = 0$ the correlation function gives the normally ordered fluctuations of the homodyne field, which in this case show a logarithmic-type divergence, when threshold is approached:

$$\lim_{r/\xi_{1,2} \to 0} C(r, \tau = 0) \sim -\ln \left(I_{0s}^{(thr)} - I_{0s} \right). \quad (115)$$

D. Frequency behavior of the spatial correlation function

Instead of the equal-time spatial correlation function, we can consider another quantity which is more easily measured in an experiment, namely, the spatial correlation function in the frequency domain defined by Eq. (36). In terms of the normalized frequency $\overline{\omega}$ the spatial correlation function $\tilde{C}(\mathbf{r}, \overline{\omega})$ is defined as

$$\tilde{C}(r, \overline{\omega}) = L_1^2 \tilde{\Gamma}(\mathbf{r}, \overline{\omega}) = \int \frac{d^2\mathbf{q}}{(2\pi)^2} \cos(\mathbf{q} \cdot \mathbf{r}) S(q, \overline{\omega}). \quad (116)$$

Figure 7 shows the spatial spectrum of squeezing $S(q, \omega)$ for $\phi_L = \pi/2$, $\mathcal{A}_{0s} = 0.95$, $\omega = 0$, and (a) $\Delta_1 = 0$, (b) $\Delta_1 = -1$. Note that this spectrum for fixed phase ϕ_L looks quite different (apart from a small neighborhood of $q = q_c$) from the optimized spectrum shown in [16], in which for each wave vector q one selects a different phase ϕ_L which optimizes the level of squeezing for $\omega = 0$. As a matter of fact, in the spectrum for fixed ϕ_L the region of q where there is squeezing becomes narrower and narrower as the OPO threshold is approached, whereas in the optimized spectrum it remains broad.

By comparison of Figs. 3 and 7 we see also that for $\phi_L = \pi/2$, $S(q, \overline{\omega} = 0)$ is mostly positive, whereas $S(q, \tau = 0)$ is negative for all values of q. The quantity $\tilde{C}(r, \overline{\omega} = 0)$ can be again computed in terms of modified Bessel functions of first and zero order, and it is shown in Fig. 8, for $\Delta_1 = -1$ and $\phi_L = \pi/2$.

Most of the properties of the equal-time correlation function are preserved, namely,

(1) when Δ_1 is negative, this correlation function has a spatial modulation with a wavelength identical to that of the pattern which appears above threshold;

(2) the function is exponentially damped at large distance, and the correlation length diverges approaching the threshold with a power law

$$\xi \sim (I_{0s}^{thr} - I_{0s})^{-\nu}$$

$$\text{with} \quad \begin{cases} \nu = 1/4 & \text{for} \quad \Delta_1 = 0 \\ \nu = 1/2 & \text{otherwise} \end{cases} . \tag{117}$$

XI. CONCLUSIONS AND COMMENTS

In the first part of this article, i.e., in Secs. II–IV and VII, we have formulated a general operational theory to describe the spatial structure of squeezed states. We have shown, especially, that the need for using a local oscillator field with variable spatial configuration can be circumvented by measuring appropriate spatial correlation functions of the electric field [10,24,29–31]. This can be obtained by using either a pair of pointlike detectors with variable position, or a CCD camera (more precisely, by two correlated pairs of detectors or by two correlated CCD cameras, because one must detect simultaneously the two beams B_1 and B_2 in Fig. 1).

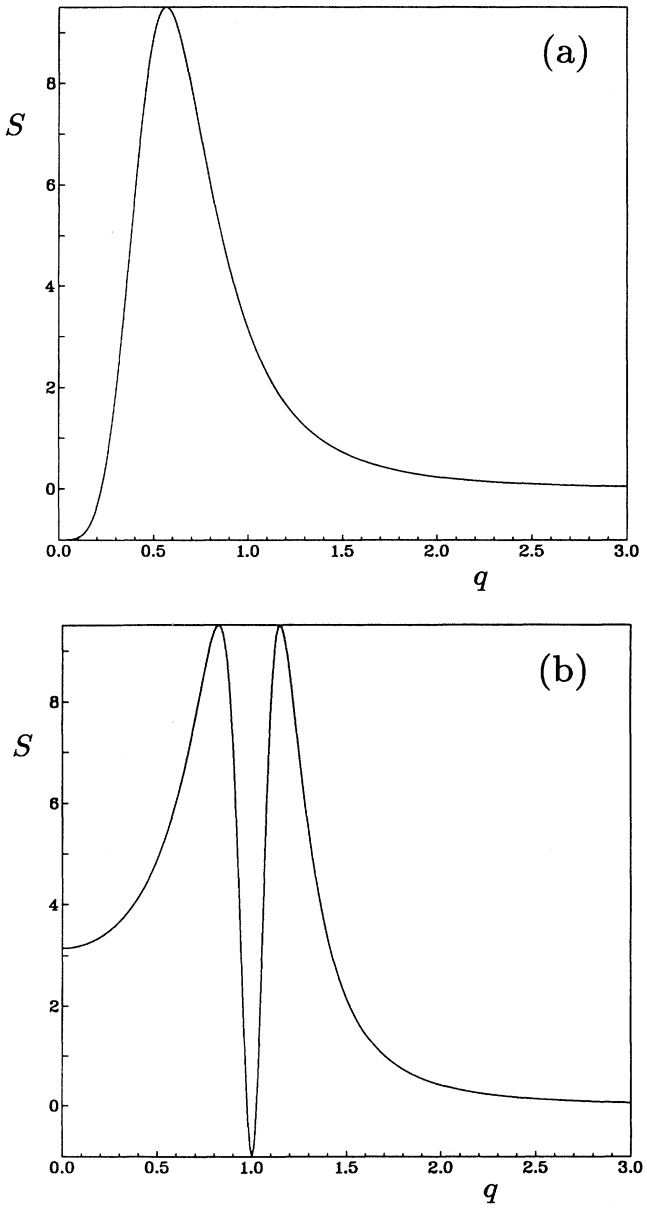

FIG. 7. The spatial spectrum of squeezing $S(q,\bar{\omega})$ is plotted as a function of q for $\bar{\omega} = 0$, $\phi_L = \pi/2$, $\mathcal{A}_{0s} = 0.95$, and (a) $\Delta_1 = 0$, (b) $\Delta_1 = -1$. Note that this spectrum for fixed phase ϕ_L looks quite different (apart from a small neighborhood of $q = q_c$) from the optimized spectrum shown in [16].

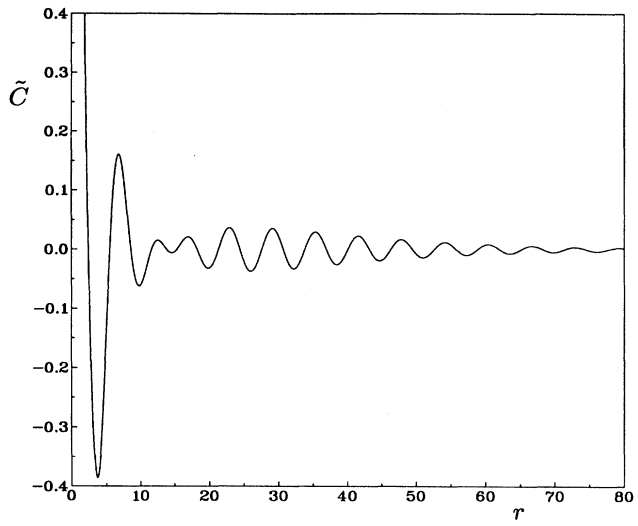

FIG. 8. Zero-frequency spatial correlation as a function of the scaled distance r, for $\Delta_1 = -1$, $\phi_L = \pi/2$, and $\mathcal{A}_{0s} = 0.99$. One can note the spatial modulation, and the fact that $\tilde{C}(r = 0, \bar{\omega} = 0)$ is positive (actually diverging at threshold).

In the second part we focused on the case of a simple quantum model which describes a degenerate optical parametric oscillator with plane parallel mirrors, below threshold. Especially, we analyzed the critical behavior that emerges when the threshold of the OPO is approached. The correlation length turns out to diverge at the critical point, and this result completes ideally the well known analogy with a second-order phase transition [17–19], by adding to the analysis the necessary spatial aspects.

Under conditions of negative detuning Δ_1, the spatial correlation function below threshold exhibits a modulation identical to that which appears in the intensity distribution above the OPO threshold. This phenomenon provides an example of the quantum image [15,24], i.e., a noisy image in which the spatial distribution of both intensity and phase is uniform, at least on average, but the observation of the spatial correlation function of the electric field quadratures reveals a regular modulated structure [32]. An extended discussion of this concept can be found in [15]. The behavior of the spatial correlation function shows a dramatic phase dependence, as well expected, and especially exhibits a definite signature of the quantum nature of the noise in the fact that, in the

squeezed quadrature component $\phi_L = \pi/2$, for small distances the equal–time correlation function takes negative values.

In the OPO below threshold the signal field is exactly zero in the semiclassical picture. Hence the signal field is purely generated by quantum noise and, under the condition of negative detuning, quantum noise creates an image which can be observed via the space correlation function. A quantum image is met also above threshold, in a "mesoscopic" OPO with reduced photon number [15]. In this case quantum noise destroys the classical image (stripe intensity pattern) and what remains is a quantum image. In the model of the OPO below threshold that we analyze here it is not necessary to reduce the physical dimensions of the OPO to obtain a quantum image, because the number of photons is not huge.

In a future work, we plan (1) to analyze the effect of a breaking of the translational symmetry in the system, as was done in [15] for the OPO above threshold, and especially (2) to study the more standard case of an OPO with spherical instead of plane mirrors.

ACKNOWLEDGMENTS

We are grateful to Andrea De Marchi for his suggestion to analyze the space correlation function, and to Philippe Grangier, Hermann Haken, Mikhail Kolobov, Lorenzo Narducci, and Marlan Scully for stimulating discussions. This research was carried out in the framework of the Esprit Basic Research Projects No. 6934 QUINTEC and No. 7118 TONICS, and of the Human Capital and Mobility Network No. 920887 "Nonclassical light."

APPENDIX

Let $f_l(\mathbf{x})$ be a complete set of orthonormal modes, where l indicates an appropriate set of indices. Let us consider the expansion

$$\langle A_{out}(\mathbf{x})\rangle = \sum_l c_l f_l(\mathbf{x}) \,, \tag{A1}$$

where $\langle\,\rangle$ indicates the mean value, and a LOF of the form

$$\alpha_L(\mathbf{x}) = f_l(\mathbf{x}) e^{i\eta} \,, \tag{A2}$$

where η is an arbitrary phase. Using Eq. (5) and the orthonormality of modes f_l, we obtain

$$N^{\frac{1}{2}} \langle E_H\rangle = 2\sigma_l \cos(\zeta_l - \eta) \,, \tag{A3}$$

with

$$\sigma_l \exp(i\zeta_l) = c_l \,. \tag{A4}$$

Hence, if one varies η until $N^{\frac{1}{2}}\langle E_H\rangle$ assumes its maximum value, one has that

$$\zeta_l = \eta \tag{A5}$$

and

$$\sigma_l = N^{\frac{1}{2}}\langle E_H\rangle/2 \,. \tag{A6}$$

[1] *Transverse Effects in Nonlinear Optical Systems*, edited by N. B. Abraham and W. J. Firth, special issue of J. Opt. Soc. Am. B **7**, 948 (1990); **7** 1264 (1990).
[2] L. A. Lugiato, Phys. Rep. **219**, 293 (1992).
[3] C. O. Weiss, Phys. Rep. **219**, 311 (1992).
[4] *Nonlinear Optical Structures, Patterns and Chaos*, edited by L. A. Lugiato, special issue of Chaos, Solitons Fractals, **4**, 1251 (1994).
[5] *Squeezed Light*, edited by R. Loudon and P. L. Knight, special issue J. Mod. Opt. **34**, 703 (1987); see expecially the introductory article by the editors.
[6] *Squeezed States of the Electromagnetic Field*, edited by H. J. Kimble and D. F. Walls, special issue of J. Opt. Soc. Am. B **4**, 1450 (1987).
[7] *Quantum Noise Reduction in Optical Systems/Experiments*, edited by C. Fabre and F. Giacobino, special issue of Appl. Phys. B **55** (1992).
[8] H. P. Yuen and J. H. Shapiro, IEEE Trans. Inf. Theor. **IT-24**, 657 (1978).
[9] J. H. Shapiro, IEEE J. Quantum Electron. **QE–21**, 237 (1985).
[10] M. I. Kolobov and I. V. Sokolov, Zh. Eksp. Teor. Fiz. **96**, 1945 (1989) [Sov. Phys. JETP **69**, 1097 (1989)]; Phys. Lett. A **140**, 101 (1989); Europhys. Lett. **15**, 271 (1991).
[11] A. La Porta and R. E. Slusher, Phys. Rev. A **44**, 2013 (1991).
[12] P. Kumar and M. I. Kolobov, Opt. Commun. **104**, 374 (1994).
[13] L. A. Lugiato and F. Castelli, Phys. Rev. Lett. **68**, 3284 (1992).
[14] G. Grynberg and L. Lugiato, Opt. Commun. **101**, 69 (1993).
[15] L. Lugiato and G. Grynberg, Europhys. Lett. **29**, 675 (1995).
[16] L. A. Lugiato and A. Gatti, Phys. Rev. Lett. **70**, 3868 (1993).
[17] V. Degiorgio and M. O. Scully, Phys. Rev. A **2**, 1170 (1970).
[18] R. Graham and H. Haken, Z. Phys. **237**, 31 (1970).
[19] H. Haken, *Synergetics–An Introduction* (Springer-Verlag, Berlin, 1977).
[20] R. J. Glauber, Phys. Rev. **130**, 2529 (1963); **131**, 2766 (1963).
[21] P. D. Drummond, K. J. McNeil, and D. F. Walls, Opt. Acta **28**, 211 (1981).
[22] P. D. Drummond, K. J. McNeil, and D. F. Walls, Opt.

Acta **27**, 321 (1980).
[23] G. L. Oppo, M. Brambilla, and L. A. Lugiato, Phys. Rev. A, **49**, 2028 (1994); G.-L. Oppo, M. Brambilla, D. Camesasca, A. Gatti, and L. A. Lugiato, J. Mod. Opt. **41**, 1151 (1994).
[24] P. L. Knight *et al.* (unpublished).
[25] L. A. Lugiato, C. Oldano, C. Fabre, E. Giacobino, and R. Horowicz, Nuovo Cimento D **10**, 959 (1988).
[26] G. Nicolis and I. Prigogine, *Self-Organization in Nonequilibrium Systems* (Wiley, New York, 1977).
[27] M. J. Collett and D. F. Walls, Phys. Rev. A **32**, 2887 (1985); C. M. Savage and D. F. Walls, J. Opt. Soc. Am. B **4**, 1514 (1987).
[28] See, e.g., *Handbook of Mathematical Functions*, edited by M. Abramowitz and I. Stegun (Dover Publ., New York, 1970), pp. 374–388.
[29] H. Heidmann, S. Reynaud, and C. Cohen-Tannoudji, Opt. Commun. **52**, 235 (1984).
[30] H. Heidmann and S. Reynaud, J. Phys. (Paris) **46**, 1937 (1985).
[31] D. F. Smirnov and A. S. Troshin, Usp. Fiz. Nauk **153**, 233 (1987) [Sov. Phys. Usp. **30**, 851 (1987)].
[32] More in general, in the definition of quantum image one must replace the sentence "uniform spatial distribution" by "trivial spatial distribution," where "trivial" means, e.g., the prefixed radial configuration of a Gauss-Laguerre mode.